Transient Behavior of Liquid Jets Injected Normal to a High-Velocity Gas Stream

D. M. Less* and J. A. Schetz†
Virginia Polytechnic Institute and State University, Blacksburg, Virginia

The transient effects of the breakup and atomization of liquid jets in a crossflow on the size of droplets within the plume were experimentally determined. Water and water/methanol mixtures were injected normal to an air stream at Mach numbers 0.48 and 3, at ambient temperature and at stagnation pressures of 1.4 and 4.3 atm, and at liquid-to-gas momentum flux ratios from 4–12. Droplet size distributions at sampling rates of up to 9 kHz were obtained using a Fraunhofer diffraction technique. The transients in the liquid mass flow rates were inferred from measurements of the extinction of a laser beam passing through the aerosol. The droplet sizes were found to fluctuate with frequencies of the order of 1–15 kHz. The fluctuations were characterized by a sudden and relatively brief increase in the mean diameter of the droplets caused by the passage of fractured clumps. Also evident was the very small size of the droplets that had been sheared off the windward surfaces of the jet. The jet fracture frequency was related to the frequency of waves propagating along the initial jet column. The axial column waves are postulated to have been caused by jet perturbations created by vortices in the air flow around the jet column.

Nomenclature

d,D = diameter
h = penetration height
M = Mach number
N = frequency
P_0 = stagnation pressure
$\bar{q}$ = momentum flux ratio, $\equiv \rho_j V_j^2/\rho_\infty V_\infty^2$
Re = Reynolds number, $\rho V d/\mu$
U,V = velocities
We = Weber number, $\equiv \rho V^2 d/\sigma$
x,y,z = coordinates
μ = viscosity
ρ = density
σ = surface tension

Subscripts

F = fracture
g = gas
j = initial jet conditions
ℓ = liquid
o = orifice
W = wave

Introduction

THE injection of a liquid jet into a high-velocity crossflow is dominated by several high-frequency processes. Although these processes have been documented in the literature, their influence on the resulting droplet size distribution has been heretofore unknown. Transients in the size of the droplets can greatly influence the effectiveness of fuel injection and combustion, as well as cooling sprays, the major applications of this work.

Liquid injection into a crossflow of air has been previously studied in numerous investigations (e.g., Refs. 1–14). From these works, a model of the jet plume has been devised; Fig. 1 is a schematic of this model. Initially, the liquid forms a circular, coherent column. As the liquid penetrates the crossflow, axial waves develop along the surface of the jet column and propagate along the plume with increasing amplitude and speed. The plume curves downstream due to aerodynamic drag and eventually fractures at the trough of a high-amplitude wave. Aerodynamic forces quickly decompose the liquid fragment. This region of the jet plume is referred to as the spray formation zone. The spray then becomes atomized within a short distance. In the atomization zone, the droplets mix with the turbulent air flow. Droplets are also shed off the outer, windward surface of the jet; these very small droplets form an outer core of the jet plume.

In Refs. 1–3, the high-frequency processes were observed and measured by high-speed motion pictures and rotating mirror camera photographs. The amplitude and speed of the axial waves were documented. Even close to the injector, the waves were propagating at speeds significantly larger than that of the liquid. These tests, performed with a supersonic crossflow, demonstrated the violence of the fracture process. In fracturing, a clump of liquid would snap away from the main jet body in a whipping-like motion. For the injection conditions tested, the jet fractured at rates of 1–18 kHz. The frequency of the axial waves was several times higher, since not every wave trough produced a fracture of the main jet body.

An important parameter related to the behavior of the jet plume is the dynamic pressure ratio, $\bar{q}=\rho_j V_j^2/\rho_\infty V_\infty^2$. High $\bar{q}$ jets ($\bar{q}\geq 6$) have well-defined jet columns. Low $\bar{q}$ jets ($\bar{q}\leq 1$), however, break up immediately upon injection, and the liquid is quickly swept downstream. Jets with an intermediate value of $\bar{q}$ exhibit features of both high and low $\bar{q}$ jets. In general, the main droplet size has been found to decrease with increasing $\bar{q}$ over the range of $\bar{q}$ tested in these previous investigations ($1\leq\bar{q}\leq 16$).

The main thrust of this paper was to quantitatively characterize the time-dependent behavior of a liquid jet in a gaseous crossflow. The droplet size distribution of the spray was measured by laser beam scattering at rates of up to 9 kHz. The frequency of fluctuations in the jet plume was determined by measuring the time rate of change of the transmission of a laser beam passing through the plume.

Received April 26, 1985; revision received April 14, 1986.

*Graduate Research Assistant, Aerospace and Ocean Engineering Department. Student Member AIAA.

†Professor and Department Head, Aerospace and Ocean Engineering Department. Fellow AIAA.

Complete details on apparatus, methods, uncertainty analysis, results, and a comprehensive discussion of the results are available in Ref. 22. Space limitations allow a discussion of only the major findings here.

Experimental Apparatus and Procedure

Facility and Models

The tests were performed in a 23×23 cm (9×9 in.) supersonic blow-down tunnel at ambient stagnation temperature. The supersonic crossflow trials were at Mach 3 at a stagnation pressure of 4.3 atm ± 1.5%. The stagnation pressure was 1.4 atm ± 10% for the Mach 0.48 tests. Interchangeable test sections allowed the tunnel to be operated at both supersonic and subsonic air velocities.

Two liquids were injected using a pressurized injection system—a 10% methanol/water mixture and pure water. The density of the mixture was 0.98 g/ml, the viscosity was 1.005 cP, and the surface tension was 58 dyne/cm. The respective properties of the water were 1 g/ml, 1 cP, and 73.5 dyne/cm.

For the supersonic tests, the liquids were injected through a flat plate model with dimensions of $10 \times 15.25 \times 0.8$ cm. The orifice was 8 cm downstream of the sharp leading edge, and it had a diameter of 0.508 mm (1/50 in.), a 1.6 mm straight run, and a smooth conical entry. An injector was mounted in the floor of the subsonic test section. The orifice had a 0.91 mm diam (1/28 in.) and a short straight run preceded by a conical entry.

Droplet Sizing System

A droplet sizing instrument was designed and built in the laboratory. A commercially available droplet sizing system could not have operated at the high frequencies required for this experiment, thus predicating a custom design. The system was developed using the principles of Fraunhofer diffraction, as outlined in Refs. 15–18.

A 5 mW helium-neon laser beam was directed into the test section. The beam was spatially filtered and expanded to a diameter of about 1 mm. High quality windows were installed on both sides of the test section, inside which the beam was diffracted by droplets in the jet plume. A plano-convex lens, 5.2 cm in diameter with a focal length of 50 cm, converged the diffracted beam onto the detector. All of the optics were mounted on optical benches, allowing the system to be positioned at a variety of x/d and z/d locations. As defined by Fig. 1, x/d and z/d are the jet plume coordinates normalized by the injector diameter.

A high-speed video camera using a CCD (charge coupled device) detector measured the intensity of the diffraction pattern along a radial line. The pattern was assumed to be radially symmetric. The solid state sensor consisted of a linear array of 2048 pixels located on 15 μm centers. The equivalent ASA of the device was slightly less than 100, and the CCD possessed a dynamic range of 5000:1 relative to RMS noise.

The data from the CCD was collected, stored on disk, and reduced by a microcomputer. A tracking-type ADC board sampled the data with digitization rates of up to 3.5 MHz. The data acquisition system had an absolute accuracy of ± 1% and a slew rate of 4 V/μs. High speed op amps were installed at the inputs for offset control and signal conditioning.

The entire system was operated at data rates ranging from 1 to 20 MHz and with CCD exposure times of 0.1 to 60 ms. Each exposure was essentially a video photograph of the diffraction pattern from which the droplet size distribution could be inferred. Data from 270 and 350 pixels were used to calculate each size distribution. Since the ADC memory held only 1024 data points, only three size distributions could be recorded consecutively. Hence, at the fastest speed, three sequential measurements could be made over a period of 0.3 ms.

The accuracy of the system was checked by a calibration reticle. Under conditions similar to those during testing, the calculated Rosin-Rammler parameters $\bar{x}$ and n, denoting the mean diameter and the spread of the distribution function, respectively, were within 6% of their true values.

Droplet Sizing Errors

Several different types of errors can affect the measurements. They will be individually discussed, beginning with optical filtering. In optical filtering, the converging lens acts as a Fourier transform lens. Because of its finite-clear aperture size, the lens filters out the high spatial frequency information produced by very small droplets. For the optical arrangement used in this experiment, the first maximum of the diffraction produced by a 7 μm diam droplet should pass through the aperture of the lens. The system was designed to measure droplets in the 7 to 100 μm diam range.

Another source of error, beam steering, arises when gradients occur in the index of refraction of the gaseous medium. These gradients generally occur in the vapor envelopes surrounding evaporating or combusting droplets, but the liquids used in this work do not show any appreciable evaporation at the conditions of static temperature and pressure tested. A shock wave can steer the beam as well. Additionally, a shock wave can also bring the diffraction pattern to focus in a plane other than the focal plane of the lens. The position of the central, undiffracted portion of the beam was verified for each run and no sign of beam steering was ever detected within the resolution of the system. The setup was also checked for an out-of-focus diffraction pattern; none was found.

Multiple scattering occurs when the spray is densely populated. Previous investigators have correlated the errors of multiple scattering with the transmission/extinction of the illuminating beam.[19] Using the correlations delineated by

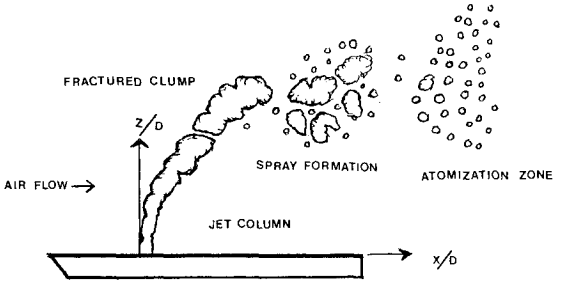

Fig. 1 Schematic of liquid jet in gaseous crossflow.

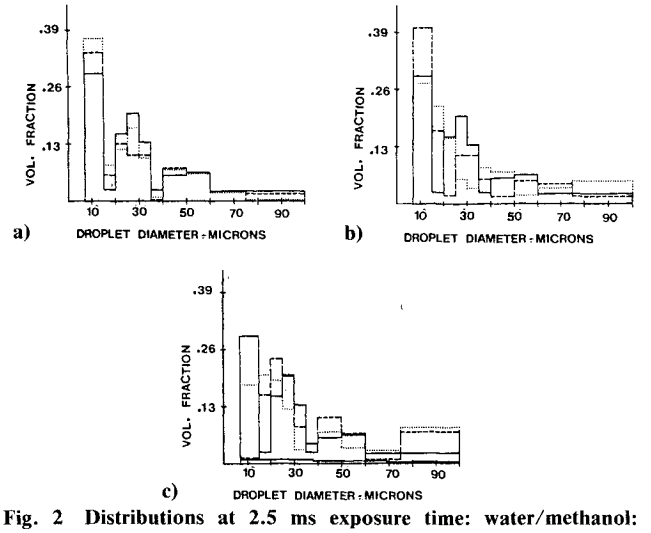

Fig. 2 Distributions at 2.5 ms exposure time: water/methanol: $\bar{q} = 12$; $M = 3$.

Dodge,[20] the multiple scattering errors in the Sauter Mean Diameter (SMD) and the Rosin-Rammler parameters should be less than 5% for the data presented in this paper.

Close to the injector, some of the droplets may not be spherical. These droplets would be incorrectly sized by the system since the computer algorithm assumes that all the droplets are spherical. Short exposure photographs taken of similar jet plumes[1-4] indicate that the vast majority of droplets are spherical at and beyond $x/d = 10$.

Frequency Measurements

To measure the frequency of the axial column waves, fracture, and other jet fluctuations, the Fourier transform lens and CCD detector were replaced by a photomultiplier tube. This setup recorded the changes in the intensity of the undiffracted portion of the laser beam. When the beam was directed through the jet plume, this system would be sensitive to changes in the number and size of droplets passing through the beam. The spray was dense enough to insure the presence of several droplets in the beam at all times, i.e., detection of the passage of individual droplets was not possible. A fast Fourier transform program searched for any periodic high frequency oscillations in the photomultiplier output signal.

Results

Injection into a Supersonic Crossflow

At every location in the jet plume, the droplet size distribution varied significantly with time. The transient behavior of the spray was dominated by the effects of jet fracture. Figures 2 and 3 present the transient droplet size distributions for a $\bar{q} = 12$ water/methanol jet in a Mach 3 crossflow at a single plume location ($x/d = 24$ and $z/d = 12$). Each plot contains two or three sequential distributions. The distribution denoted by the solid line was recorded first; the dotted line distribution was recorded immediately following; and the dashed line represents the distribution measured during a third exposure. The interval between sequential exposures was a few nanoseconds long and can be ignored.

Figure 2c shows the transients the best. The spray was most typically represented by the solid line distribution; this can be verified by comparing it with the distributions depicted in Figs. 2a and 2b. The large population in the 7-15 μm diam bin was due in part to the very small droplets that shed off the windward surface of the jet and form an outer core to the plume. These very small droplets are evident at most locations, even near the injector. The other two distributions in Fig. 2c denote the passage of droplets that resulted from a fracture of the jet column. The fractured clump has been decomposed into droplets by this downstream passage. Since the jet fractures periodically (in pulses rather than in a continuous fashion), the resulting droplets appear in only a few of the exposures.

Figure 2 was obtained by using a 2.5 ms exposure time; Fig. 3 shows the distributions with an exposure time of 0.65 ms. As the exposure time is decreased, the chance that a train of two or three sequential exposures will catch the periodic passage of the fractured droplets decreases. None of the exposures in Fig. 3 detected the presence of a significant number of 75+ micron droplets. In comparing the distributions in the two figures, it is evident that the distributions vary with a certain periodicity. The distributions in Fig. 3 resemble fragments of those contained in Fig. 2. The distributions underwent an oscillation in droplet size (small in Fig. 3a, intermediate in Figs. 3b and 3c, and large during the passage of droplets resulting from a fracture) at a frequency of about 1 kHz. Consequently, a 0.65 ms exposure (Fig. 3) provided a stop-action view of the spray while a 2.5 ms exposure (Fig. 2) partially time-averaged the fluctuations.

Table 1 quantifies these observations. For the same test conditions as in Figs. 2 and 3, the table lists the SMD and the standard deviation of SMD (normalized by the SMD) for a series of distributions recorded at various exposure times. A very long exposure produced distributions that varied little in time. The steadiness is evident in the standard deviations and in the uniformity of the recorded SMD values. Both the 0.65 and 2.5 ms trials produced substantial variations in the mean droplet diameter. The 19.7 μm SMD values recorded at 25 ms lies between the extreme SMD values (18 and 23 microns) found at these two shorter exposure times. Reducing the exposure time further seemed to reduce the standard deviation. Due to equipment limitations, these very short exposure tests consisted of only two sequential exposures. Within the 0.45 ms intervals covered by these trials, no significant variation in the droplet size was observed. This suggests that the major jet disturbance—the passage of droplets produced by a fracture—occurred only briefly. A simple statistical model indicated that the disturbance (i.e., presence of very large droplets) lasted only about 0.1 ms and was repeated once a millisecond.

Another manner of representing these fluctuations is demonstrated by Table 2. The time history of SMD, recorded at various exposure times and locations, is presented

Table 1 Mean and standard deviation of SMD for various exposure times[a]

Exposure time, ms	Set no.	SMD, μm	Standard deviation of SMD
25.0	1	19.7	0.001
5.0	1	18.4	0.09
	2	18.5	0.09
	3	18.3	0.10
	Average	18.4	0.09
2.5	1	18.7	0.06
	2	18.6	0.08
	3	22.8	0.17
	Average	20.0	0.11
0.65	1	17.6	0.07
	2	23.4	0.12
	3	23.5	0.13
	Average	21.5	0.11
0.375	1	19.1	0.01
	2	19.4	0.02
	3	19.4	0.002
	Average	19.3	0.01
0.225	1	19.3	0.003
	2	19.2	0.006
	3	19.0	0.002
	Average	19.2	0.004

[a]Water/methanol: $\bar{q} = 12$; $M_\infty = 3$; $x/d = 24$; $z/d = 12$.

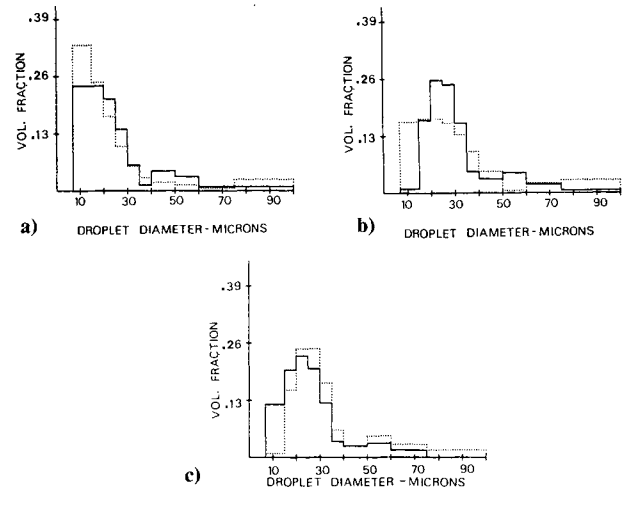

Fig. 3 Distributions at 0.65 ms exposure time: water/methanol: $\bar{q} = 12$; $M = 3$.

Table 2 Time histories of SMD for high $\bar{q}$ water jet in supersonic flow[a]

Exposure time, ms	x/d	z/d	Time history of SMD, μm
0.11	10	6	16.9, 16/ 23.4, 21.9/ 24.7, 23.1/ 18.7, 20.4/ 17.4, 17.9/ 18.8, 22.8
0.11	20	8	17.6/ 18.5/ 14.6/ 14.4/ 20.1/ 16.1
0.11	20	14	21, 18.3/ 19.2, 15.5/ 18.5, 22.6/ 26.4, 19.6/ 33.7, 19.3/ 17.2, 19.9
0.11	30	14	18.5, 18.3/ 17.2, 15.7/ 16.7, 17
0.11	40	10	19.9, 18.5/ 20.3, 27.3/ 16.3, 23.3
0.11	50	10	23.6, 16.9/ 25.9, 22.9/ 21.3, 17.9/ 23.6, 17.9/ 24.7, 27.7/ 30.2, 25.5
0.11	100	16	15.6, 18.1/ 16.1, 21.8/ 23.8, 20.1/ 22.1, 16.6/ 18.8, 30.8/ 24.7, 24.9
0.35	20	14	17.6, 18.7, 17.6/ 18.5, 20.2, 17.6/ 19.5, 18.9, 23.2
0.35	30	14	18.6, 16.7, 25.2/ 16.7, 17, 17.3/ 15.6, 16.5, 21
2.7	10	6	17.8, 17.5, 20.9, 18.5, 21.8, 19.9/ 18.5, 26.2, 22.4
2.7	20	8	15.9, 19.6, 15.5/ 17.8, 15.3, 19.6/ 20, 14, 21
2.7	40	10	15.1, 16.7, 20.2/ 16.8, 27.8, 27.3/ 20.5, 26.9, 27.1
2.7	60	16	18.2, 19.1, 22.7/ 22.2, 25.9, 18.3/ 25.5, 25.4, 17
25	20	16	19.9/ 18.7/ 18.2
25	30	16	19.7/ 18.9/ 19.8
25	50	10	19.4/ 19.6/ 20
25	100	20	19.2/ 20.5/ 19.9

[a] Water: $\bar{q}=10$; $M_\infty=3$.

for a $\bar{q}=10$ water jet. A comma separates sequential readings, while a slash separates different tests. For a long exposure time, the SMD was nearly constant. At exposure times of 0.35 and 2.7 ms, the mean diameter ranged from 17 to 30 μm. The SMD value, however, was usually close to 17μm.

Two significant differences were noted between the water and the water/methanol jets. At the 25 ms exposure time, the standard deviation in SMD for the water jet (0.046) was an order of magnitude larger than that recorded for the methanol mixture. The water jet also fluctuated at a higher frequency than the water/methanol jet at the same $\bar{q}$. The variation in the 0.11 ms trials listed in Table 2 indicates that the water jet must have fractured at a frequency noticeably higher than the 1 kHz frequency observed for the methanol mixture jet.

As the droplets progress downstream, they are gradually atomized by aerodynamic forces. The 0.11 ms distributions in Fig. 4 clearly demonstrate the gradual decrease in the droplet diameters with increasing downstream distance. Generally, the standard deviation in the SMD was large in the spray formation zone and gradually decreased throughout the atomization zone. The boundary between the spray formation zone and the atomization zone, $x/d\simeq 30$ for $\bar{q}=4$ and $x/d\simeq 40$ for $\bar{q}=12$, was identified through high-speed movies and photographs taken during previous investigations (Refs. 1-4).

Table 3, recorded for a $\bar{q}=4$ water jet, tabulates the populations of droplet diameters within three groupings. Two distributions are listed for each entry; they represent the distributions found at observed extreme values of the SMD. The 0.35 ms entries again demonstrate the gradual shift toward smaller diameters with increasing downstream

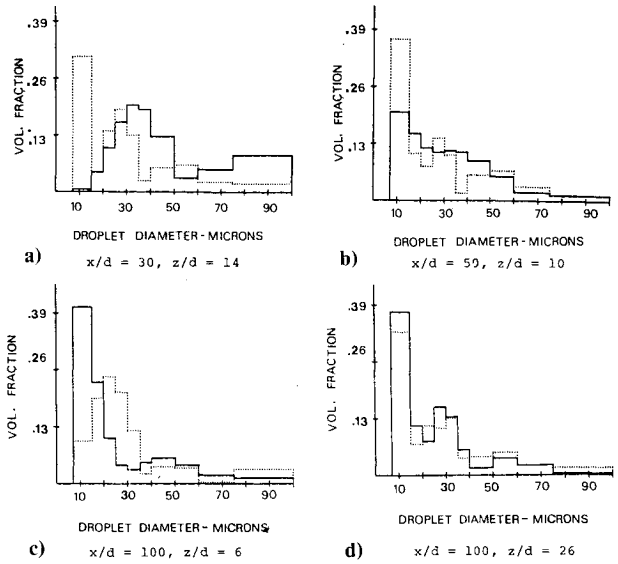

Fig. 4 Various distributions at 0.11 ms exposure: water: $\bar{q}=10$; $M=3$.

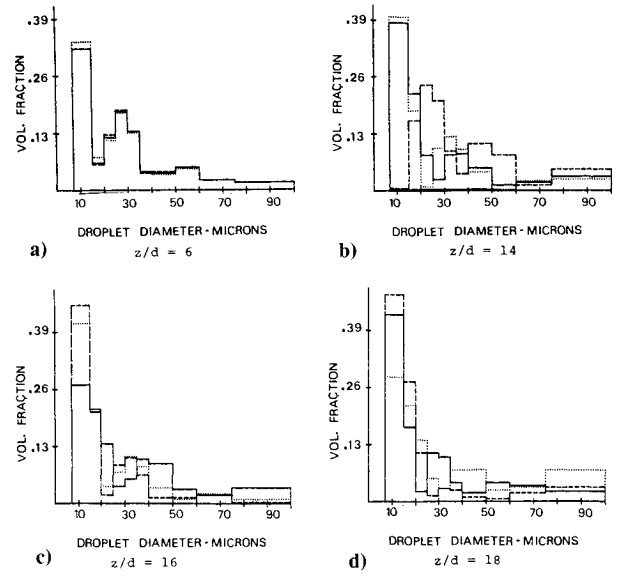

Fig. 5 Distribution at various z/d: water: $\bar{q}=10$; $M=3$; 2.7 ms exposure; $x/d=30$.

distance. At $x/d=20$ and 40, the 2.1 ms entries appear to be averages of the 0.35 ms entries at the same locations. Further downstream, however, the 2.1 ms exposure detected large fluctuations in the droplet size distributions. The frequency of these fluctuations must have been of the order of tenths of a kilohertz. This observation correlates with the relatively large standard deviations in the SMD that were found for water jets when a long exposure time was used.

Kush and Schetz[2] described the water jet as a violent whipping phenomenon in which the jet column appeared to snap and toss clumps of liquid downstream. Possibly, this whipping is responsible for the previously mentioned low frequency (tenths of a kilohertz) fluctuations. In its whipping motion, the jet may disperse the fractured clumps of liquid at various z/d heights. At times, it could dispense the large droplets at large values of z/d and then at lower heights. A long exposure measurement taken far downstream would sense the fluctuations caused by the whipping. A short exposure test at the same location would probably miss the event (passage of large droplets) since it is short lived (0.1 ms) and occurs only once every 10 ms (assuming a whipping

Table 3 Variations in the population of the three major size groups[a]

Exposure time, ms	x/d	z/d	Population, μm 7–20	20–60	60–100
0.35	10	6	0.656	0.322	0.022
			0.127	0.818	0.055
0.35	20	6	0.729	0.245	0.026
			0.244	0.720	0.036
0.35	30	6	0.747	0.240	0.013
			0.198	0.757	0.045
0.35	40	8	0.664	0.307	0.029
			0.546	0.408	0.046
2.1	20	8	0.391	0.574	0.035
			0.326	0.631	0.043
2.1	40	8	0.406	0.555	0.039
			0.259	0.680	0.061
2.1	50	8	0.596	0.273	0.131
			0.181	0.568	0.251
2.1	100	10	0.697	0.200	0.103
			0.170	0.741	0.089

[a]Water: $\bar{q}=4$; $M_D=3$.

frequency of 0.1 kHz). Subsequent analysis of the high speed movies taken for Ref. 2 revealed that each fracture dispersed droplets throughout the plume (in the z direction), however, the main fractured fragment was directed downstream at varying z/d heights.

Figure 5 demonstrates how the distributions varied with z/d for a 2.7 ms survey of a $\bar{q}=10$ water jet at $x/d=30$. The $z/d=6$ plot probably represents droplets shed off the jet column, since the fractured droplets are generally dispersed at larger values of z/d (such as in Fig. 5b). As z/d increases, the populations in the 7 to 20 μm bins increase significantly. For water jets, the standard deviation in the SMD peaked at a height of $z/h\simeq 0.4$, where h denotes the penetration height of the jet plume at a given downstream location.

The frequency of the fluctuations was determined more precisely by the transmission/extinction tests. To produce Fig. 6a, a laser beam was shined through the plume of a $\bar{q}=10$ water jet at $x/d=40$, $z/d=10$. The plot depicts how the intensity of the beam was affected by fluctuations in the spray. There is some obvious periodicity to the fluctuations in the signal. When a wide range FFT was performed on the signal, almost all of the observable activity occurred at frequencies of less than 30 kHz (Fig. 6b). Figure 6c shows that the activity is centered between 1 and 10 kHz. Fast Fourier transforms performed at smaller frequencies determined that the amplitude of the disturbances gradually decreased with frequency. The frequency of the disturbances was restrained to only a few kilohertz when close to the fracture point. Tests conducted relatively close to the injector but beyond the fracture point would be most sensitive to the affects of jet fracture. The frequencies also varied slightly with varying z/d. The highest frequencies (15–20 kHz) were found for water jets (both high and low $\bar{q}$) at a height of $z/h=0.75$.

The frequency of the main fluctuations (those caused by jet fracture) were calculated and verified by several methods, including FFT's of the transmission signal and by examination of the SMD time histories. The fluctuation frequency of the high $\bar{q}$ water/methanol jet was determined to be slightly less than 1 kHz. The water jet fluctuated at frequencies of 4 and 1 kHz, respectively, for high and low values of $\bar{q}$ ($\bar{q}=12$ and 4). For the water jet, the whipping fluctuations were extremely aperiodic but seemed to be of the order of tenths of a kilohertz.

The largest amplitude in the transmission/extinction signal occurred at 0.4h, where, of course, the largest standard deviations in the SMD were recorded. The largest extinction of the beam was measured at heights of $z/d=5$ to 10 and

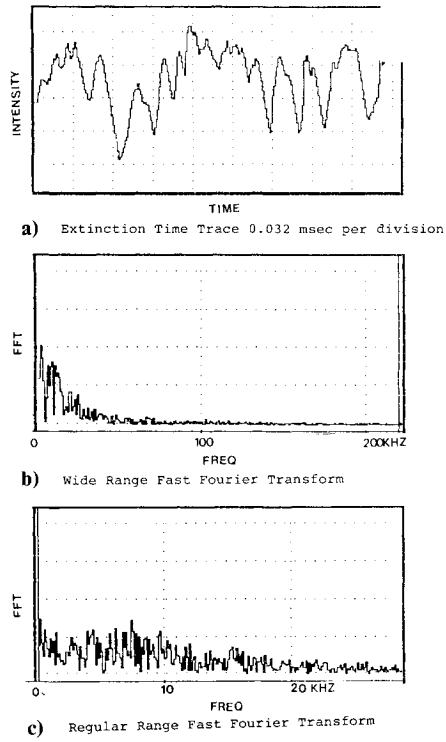

Fig. 6 Examples of extinction data: water: $\bar{q}=10$; $M=3$; $x/d=40$; $z/d=10$.

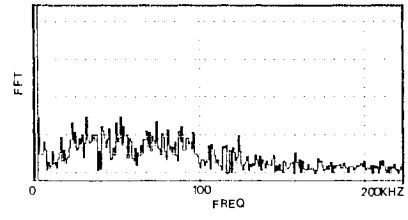

Fig. 7 Frequency spectrum at $x/d=100$; $z/d=25$: water: $\bar{q}=10$; $M=0.48$.

$z/d=10$ to 20, respectively, for the low and high $\bar{q}$ water jets at $x/d=20$. A large extinction should denote a high local liquid flow rate.

Injection into a Subsonic Crossflow

The behavior of a liquid jet in a subsonic crossflow is markedly different than that of a jet in a supersonic crossflow. In a subsonic crossflow, the jet is not violently sheared off by the crossflow; rather, the jet expands uniformly and breaks off at the trough of a column wave. The subsonic cases are not subject to the violence associated with injection into a supersonic crossflow.

Figure 7 is an example of an FFT of the extinction signal from the subsonic crossflow tests. The frequency spectrum is centered around 60 kHz, the frequency of the axial column waves. The extinction measurements must have detected the influence of jet column waves on the passage of the droplets and/or the influence of vortices in the air flow. Close to the fracture point, the FFT's detected a small peak around 15 kHz, the apparent fracture frequency. Photographs of the jet showed that, on the average, each fractured segment contained four column waves, thus explaining the 4:1 factor between the wave and the fracture frequency. Furthermore, the extinction signal traces (Fig. 8) contain a pattern which was repeated at a frequency of 15 kHz. Each pattern, the start of which is denoted by a symbol in the figure, was seemingly composed of a group of four extinction peaks. This high frequency precluded the droplet sizing apparatus (which operated at a maximum of 9 kHz) from obtaining anything

Table 4 Frequencies of jet column waves

Liquid	M	D_j, cm	Wave exp.	Freq. Eq. (1)	kHz Eq. (2)	$\bar{q}$	U_j, cm/s	$P_{\text{dyne/cm}^2}$
Water[a]	2.4	0.079	92	42	106	11	4450	345000
Water[a]	2.4	0.079	86	42	97	5	2926	345000
Water[a]	2.4	0.159	56	21	46	3	2134	345000
CS_2[a]	2.4	0.159	61	21	47	4	2743	345000
Water[a]	4	0.159	65	17	53	2	1829	966000
Water[b]	3	0.096	78	31	82	10	3900	414000
Water/alc.[b]	3	0.096	69	31	63	10	3900	414000
Water/gly.[b]	3	0.096	46	31	36	10	3900	414000
Water[d]	0.48	0.091	61	33	52	10	1907	135000
Water[c]	3	0.096	72	31	82	10	3900	414000
Water/alc.[c]	3	0.096	40	31	52	1.5	1500	414000
Water/alc.[c]	3	0.096	61	31	59	5	2800	414000
Water/alc.[c]	3	0.096	93	31	63	10	4000	414000
Fluorinert[c]	3	0.096	30	31	66	5	2100	414000
Fluorinert[c]	3	0.096	91	31	75	17	3800	414000
Water/gly.[c]	3	0.096	89	31	24	5	2500	414000
Water/gly.[b]	3	0.096	37	31	30	10	3900	414000

[a]From Ref. 2. [b]From Ref. 14. [c]From Ref. 4. [d]From present study.
N.B.: Wave frequency Eq. (1) $N_w = 0.4\ U/d$; and Eq. (2) $N_w = 0.00002\ U/d_j\ \sqrt[3]{6 V_j P_{o\infty}/\mu_\ell \rho_\ell}$.

but a time-averaged description of the aerosol for injection into a subsonic crossflow.

Discussion

Jet Column Waves

A model of the behavior of a liquid jet in a crossflow (for $\bar{q} > 1$) was developed using data obtained in this and prior investigations. The first piece of the model is concerned with the frequency of the axial waves that propagate along the jet column. Table 4 contains a partial listing of the observed jet column wave frequencies, N_w, and related test conditions. Comparing cases in which only the gas velocity and the jet diameter terms were varied, the wave frequency varied as

$$N_w = 0.4\ U/d$$

where the velocity was equal to that of the air flow striking the jet column. For the supersonic cases, this velocity was approximated by the velocity following a normal shock (a bow shock develops upstream of the jet plume; it is nearly normal directly upstream of the jet column). The diameter is the same as that of the orifice. Near the injector, where the waves first appear, the jet column has the same diameter. This relation is illuminating, since it is similar to the Strouhal equation for the flow past rigid cylinders. The usual constant for the Strouhal equation is 0.2, but that is for a pair of shedding vortices. The above equation, therefore, yields the frequency of vortices shed off a rigid cylinder having the same diameter as the liquid jet and subjected to the same crossflow. The vortices are shed for rigid cylinders only for a certain range of Reynolds numbers. The test cases listed in Table 4 all lie within the region of the von Kármán vortex street flow. On the average, the Reynolds number was 1×10^5. Similar vortices have been associated with gas jets in a crossflow (see Refs. 24–27).

There is, of course, a difference between the flow past a rigid cylinder and a cylindrical column of liquid. A strong interaction exists between the mechanics of the gas flow and the stability/deformation of the liquid column. Weber studied the stability of a liquid column in still air and determined that there was a certain wavelength of disturbance in which stability was minimized. This wavelength was proportional to $\rho_\ell \mu_\ell / \sigma$ (Ref. 21). The frequency of this disturbance should be proportional to the inverse of this quantity. The data in Table 5 was correlated into the following equation:

$$N_w = 0.00002\ \sqrt[3]{(\sigma P_{0\infty} V_j / \mu_\ell \rho_\ell)\, U/d}$$

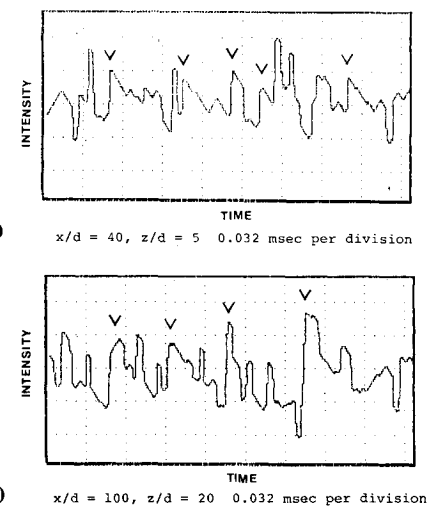

Fig. 8 Examples of extinction time traces: water: $\bar{q} = 10$; $M = 0.48$.

The units of the constant are $(\text{cm/s})^{4/3}$. Uncertainties in the exponent of the jet velocity term arose from inconsistencies in comparing the data from different reports. Each determined the wave properties using different techniques. Furthermore, previous reports listed only the wavelength and wave speed; the frequency was never directly calculated.[22]

The data from Refs. 2 and 14 indicates that the jet column waves accelerate and grow in amplitude as they propagate along the jet column. The evidence also suggests that the waves start at a velocity equal to that of the liquid and then accelerate toward the velocity of air striking the jet column. The wavelengths grow in a proportional fashion, thus the frequency of the waves is kept constant.

Jet Fracture

In a supersonic crossflow, the jet column fractures shortly behind the sonic point behind the curved bow shock and the fractured part of the column contains several axial waves.[1,2] For the case of high $\bar{q}$ water jets, four waves are usually identifiable on each fractured clump. This same number of waves per clump was also observed in the Mach 0.48 test. The number also seems to be independent of injector diameter. This number, n, can be related to the other jet

Table 5 Fracture frequencies

Liquid	D_j, cm	M_∞	$\bar{q}$	N_F, kHz	N_W, kHz	V_W, m/s	V_J, m/s	$n = N_W V_J / N_F V_W$
Water[a]	0.079	2.4	10.7	5.2	92	220	44.2	3.6
Water[a]	0.159	4	1.2	6.5	41c	157	12.2	0.5
Water[a]	0.318	2.4	0.2	4.4	29c	220	6.1	0.2
Water[b]	0.079	4	14	7	92	157	44.5	3.7
Water[c]	0.051	3	4	1-2	74c	192	24.7	4.5-9
Water[c]	0.051	3	10	4	78c	192	39	4
Water/alc.[c]	0.051	3	12	.5-1	72c	192	39	14-29
Water/gly.[d]	0.318	2.1	4.9	0.9	25c	234	17.7	2.1
Water[e]	0.091	0.48	10	15	60	—	19	4

[a]From motion pictures taken by Kush and Schetz for Ref. 2; runs 9, 16, and 13, respectively. [b]From Ref. 2, Fig. 29a. [c]From present study. Fracture frequencies from FFTS and other transient data; wave speeds calculated. [d]From Ref. 1; $\mu = 2.4$ cP. [e]From present study. Both fracture and wave frequency taken from data. The number in last column was obtained from pattern in extinction.
N.B.: Wave frequency data followed by c denotes that the frequency was calculated using equations developed in this study. Wave speed at breakup was represented by sonic velocity.

parameters as follows:

$$n = \frac{U_j}{\lambda_F N_F} = \frac{N_w U_j}{U_w N_F} \simeq \frac{N_w U_j}{U_{g,F} N_F}$$

The term $\lambda_F N_F$ is merely the length of the fractured clump. The last equality assumes that the wave speed can be approximated by the speed of the air flow striking the fracture point.

Spray Formation and Atomization

Once the spray had been atomized to a certain droplet diameter, the aerodynamic forces become balanced with the surface tension force, binding the liquid together in a spherical drop. This balance can be expressed by the Weber number. The liquid film Reynolds number represents the forces that resist the breakup of the liquid and the development of waves on the liquid surface. From this analysis and from a series of experiments, Ingebo and Foster[23] determined that the SMD varied as $(We \cdot Re_\ell)^{-0.25}$, where

$$We \cdot Re_\ell = \rho_g \rho_\ell d_o{}^2 U_g{}^3 / \mu_\ell \sigma$$

The SMD and D_{max} of the sprays tested in this and prior investigations[1-5] were parameterized into the following relation:

$$\text{SMD (microns)} = 3500\ (\mu\sigma / U_g U_j)^{0.2} (1/\rho\ell)^{1.4} \text{(cgs units)}$$

The two above relations should not be expected to be totally equivalent. The latter relation was developed from data in which $\bar{q}$ was varied between a $\bar{q}$ of 1 and a $\bar{q}$ of 16. In this range, the jet behavior changes significantly as $\bar{q}$ is changed. Ingebo and Foster tested only high $\bar{q}$ jets, consequently, they determined that the mean droplet diameter or, equivalently, the jet behavior, was independent of $\bar{q}$ and U_j.

The data indicated that D_{max} was consistently 2.8 times larger than the SMD. The quantity D_{max} was defined as the droplet diameter for which 90% of the droplets had smaller diameters. Both the SMD and D_{max} values were obtained at downstream distances of $x/d = 60$-100.

In the spray formation and the atomization zones, several processes influence the jet. The droplet size distribution is periodically disturbed by the passage of large droplets created by the fracture of the jet. Also influencing the spray are the axial waves and the vortices shed off the jet column. These latter influences are partially obscured by the violent whipping of the jet for injection into a supersonic crossflow. Also evident are the very small diameters (7-20 μm) of the droplets that are shed directly off the jet plume. Overall, the jet undergoes a variety of periodic, turbulent, and sometimes violent oscillations that directly affect the transients in the droplet size distribution.

References

[1]Sherman, A. and Schetz, J., "Breakup of Liquid Sheets and Jets in a Supersonic Gas Stream," *AIAA Journal,* Vol. 9, April 1971, pp. 666-673.

[2]Kush, E. and Schetz, J., "Decomposition of a Liquid Jet Injected Normal to a Supersonic Air Stream," AFOSR-TR-72-1180, June 1972.

[3]Schetz, J., Kush, E., and Joshi, P., "Wave Phenomena in Liquid Jet Breakup in a Supersonic Crossflow," *AIAA Journal,* Vol. 18, July 1980, pp. 774-778.

[4]Nejad, A. and Schetz, J., "Effects of Properties and Location in the Plume on Droplet Diameter for Injection in a Supersonic Stream," *AIAA Journal,* Vol. 21, July 1983, pp. 956-961.

[5]Less, D. and Schetz, J., "Penetration and Breakup of Slurry Jets in a Supersonic Stream," *AIAA Journal,* Vol. 21, July 1983, pp. 1045-1046.

[6]Thomas, R. and Schetz, J., "Mass Distribution in the Plume of a Transverse Slurry Jet in Supersonic Flow," AIAA Paper 84-0041, Jan. 1984.

[7]Weiss, C. and Worsham, C., "Atomization in High Velocity Airstreams," *ARS Journal,* Vol. 29, No. 4, April 1959, p. 252.

[8]Forde, J., Molder, S., and Szpiro, J., "Secondary Liquid Injection into a Supersonic Airstream," *Journal of Spacecraft and Rockets,* Vol. 3, No. 8, Aug. 1966, pp. 1173-1176.

[9]Reichenbach, R. and Horn, K., "Investigation of Injectant Properties on Jet Penetration in a Supersonic Stream," *AIAA Journal,* Vol. 9, March 1971, pp. 469-472.

[10]Yates, C. and Rice, J., "Liquid Jet Penetration," *Research and Development Programs Quarterly Report,* U-RQR/69-2, Applied Physics Laboratory, Johns Hopkins University, Baltimore, MD, 1969.

[11]Catton, I., Hill, D., and McRae, R., "Study of Liquid Jet Penetration in a Hypersonic Stream," *AIAA Journal,* Vol. 6, Nov. 1968, pp. 2084-2089.

[12]Gooderum, P. B. and Bushnell, D. M., "Atomization, Dropsize, and Penetration for Cross-Stream Water Injection at High-Altitude Reentry Conditions with Application to the RAM C-1 and C-III Flights," NASA TND-6747, July 1972.

[13]Padhye, A. and Schetz, J., "Penetration and Break-up of Liquid Fuel Jets in High Subsonic Speed Air Streams," AIAA Paper 77-201, 1977.

[14]Nejad, A. and Schetz, J., "Effects of Viscosity and Surface Tension of Liquid Injectants on the Structural Characteristics of the Plume in Supersonic Airstream," AIAA Paper 82-0253, Jan. 1972.

[15]Phillips, B., "A Technique for the Numerical Solution of Certain Integral Equations of the First Kind," *Journal of the Association for Computing Machinery,* Vol. 9, Jan. 1962, pp. 84-97.

[16]Twomey, S., "On the Numerical Solution of Fredholm Integral Equations of the First Kind by the Inversion of the Linear System Produced by Quadrature," *Journal of the Association for Computing Machinery,* Vol. 10, Jan. 1963, pp. 97-101.

[17]Caroon, T. and Borman, G., "Comments on Utilizing the Fraunhofer Diffraction Method for Droplet Size Distribution Measurement," *Combustion Science and Technology,* Vol. 19, 1979, pp. 255-258.

[18]Swithenbank, J., et al., "A Laser Diagnostic Technique for the Measurement of Droplet and Particle Size Distribution," AIAA Paper 76-69, Jan. 1976.

[19]Dobbins, R., Crocco, L., and Glassman, I., "Measurements of Mean Particle Sizes of Sprays from Diffractively Scattered Light," *AIAA Journal,* Vol. 1, Aug. 1963, p. 1882.

[20]Dodge, L., "Change of Calibration of Diffraction-Based Particle Sizers," *Optical Engineering,* Vol. 23, No. 5, Sept. 1984, p. 626.

[21]Lefebvre, A., *Gas Turbine Combustion,* Hemisphere Publications, Washington, D.C., 1983.

[22]Less, D., "Transient Behavior of Liquid Jets Injected Normal to a High Velocity Gas Stream," Ph.D. Thesis, Virginia Polytechnic Institute and State University, Blacksburg, VA, 1985.

[23]Ingebo, R. and Foster, H., "Drop Size Distribution for Cross-Current Breakup of Liquid Jets in Airstream," NASA TN 4087, 1957.

[24]Rajaratnam, N., "Theory of Turbulent Jets," *Handbook of Fluids in Motion,* edited by N. Cheremisinoff and R. Gupta, Ann Arbor Science, Ann Arbor, 1983, pp. 251-279.

[25]Fearn, R. and Weston, R., "Vorticity Associated with a Jet in a Cross Flow," *AIAA Journal,* Vol. 12, Dec. 1974, p. 1666.

[26]Moussa, Z., Trischka, J., and Eskinazi, S., "The Near Field in the Mixing of a Round Jet with a Cross-Stream," *Journal of Fluid Mechanics,* Vol. 80, No. 49, 1977.

[27]McMahon, H., Hester, D., and Palfrey, J., "Vortex Shedding from a Turbulent Jet in a Crosswind," *Journal of Fluid Mechanics,* Vol. 48, No. 73, 1971.